ChemComm

COMMUNICATION

View Article Online
View Journal | View Issue

Cite this: *Chem. Commun.*, 2024, **60**, 14415

Received 15th August 2024,
Accepted 4th October 2024

DOI: 10.1039/d4cc04127e

rsc.li/chemcomm

C_{sp^2}–H/F bond activation and borylation with iron†

Ethan Zars, [a] Lisa Pick, [b] Achala Kankanamge,[a] Michael R. Gau,[a] Karsten Meyer [b] and Daniel J. Mindiola *[a]

Reduction of $[K_2\{(^{tBu}pyrr_2pyr)Fe\}_2(\mu\text{-}N_2)]$ (1) with two equiv. of KC_8 in the presence of crown-ether 18-C-6 yields the N_2 adduct $[\{K(18\text{-}C\text{-}6)\}_2(^{tBu}pyrr_2pyr)Fe(N_2)]$ (2). Complex 2 heterolytically splits the C_{sp^2}–H bond of benzene to form $[\{K(18\text{-}C\text{-}6)\}(^{tBu}pyrr_2pyr)Fe(C_6H_5)]$ (3), whereby usage of a diboron B_2pin_2 promotes hydride elimination to form the salt $[K(18\text{-}C\text{-}6)HB_2Pin_2]$ (4). Similarly, 3 can also be formed by cleavage of the C–F bond of fluorobenzene. Reaction of 3 with ClBcat yields $[K(18\text{-}C\text{-}6)(thf)_2][(^{tBu}pyrr_2pyr)FeCl]$ (5) and PhBcat and the former can be reduced to 2 to complete a synthetic cycle for heterolytic benzene C–H activation and borylation.

The activation and functionalization of C–H bonds is a crucial step toward converting an unreactive and abundant substrate into more reactive or synthetically versatile functionalities.[1] Much of the early literature on C–H activation focuses on the oxidative addition of C–H bonds at low valent precious metals.[2] This research was performed in the context of cross-coupling reactions which typically go through catalytic cycles consisting of oxidative addition, transmetallation, and reductive elimination.[3] A particularly useful target for C–H functionalization would be the generation of C–B bonds due to their prevalence in Suzuki–Miyaura cross coupling reactions.[4] While C–H activation is usually accomplished with precious metals, there is precedent for this reaction at iron,[5] which is the most abundant metal in Earth's crust.[6] To this end, borylation of aryl C_{sp^2}–H bonds by photolysis of an iron boryl species has been reported,[7] with more recent studies expanding this work to catalytic processes for C–H borylation.[8] While mechanistic studies for arene C–H borylation reactions have been studied in detail with first row transition metals such as Co,[9] similar studies clearly showing the bond forming and breaking processes at the Fe center have been exceptionally rare.[5e,7b,7c,8a,8j,10]

In this contribution, we show how a formally Fe^0 and mononuclear Fe dinitrogen complex $[\{K(18\text{-}C\text{-}6)\}_2(^{tBu}pyrr_2pyr)Fe(N_2)]$ (2) ($^{tBu}pyrr_2pyr^{2-}$ = 3,5-^{t}Bu$_2$-bis(pyrrolyl)pyridine; 18-C-6 = 18-crown-6) can activate the C_{sp^2}–H bond of benzene (and the C–F bond of fluorobenzene) at room temperature to yield the ferrous phenyl complex $[\{K(18\text{-}C\text{-}6)\}(^{tBu}pyrr_2pyr)Fe(C_6H_5)]$ (3). We propose the C–H activation process to be heterolytic in nature by trapping KH with B_2pin_2 (pin = pinacolato) to form the adduct $[K(18\text{-}C\text{-}6)HB_2pin_2]$ (4). The aryl ligand from 3 can be transmetallated using ClBcat (cat = catecholato) to yield the discrete salt $[\{K(18\text{-}C\text{-}6)(thf)_2\}(^{tBu}pyrr_2pyr)FeCl]$ (5) along with the borane PhBcat (6). Finally, we show how 5 can be reduced to 2 to close a synthetic cycle for room temperature C_{sp^2}–X bond activation and borylation (Scheme 1).

We have previously shown that reduction of the ferrous precursor $[(^{tBu}pyrr_2pyr)Fe(OEt_2)]$[11] with one equiv. of KC_8 yields the formally Fe^I end-on and bridging N_2 complex $[K_2\{(^{tBu}pyrr_2pyr)Fe\}_2(\mu\text{-}N_2)]$ (1) in which the N_2 ligand bridging the two Fe centers is

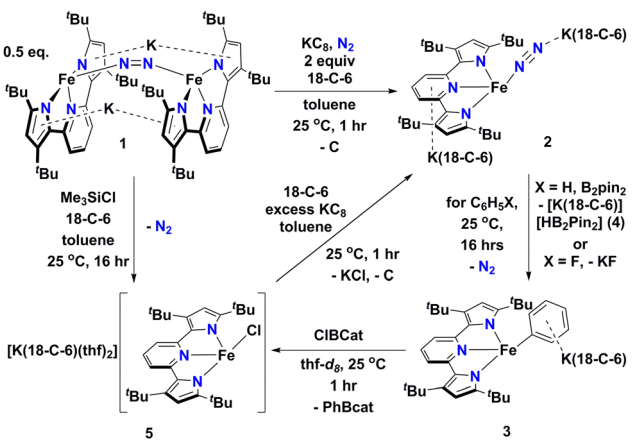

Scheme 1 Reaction scheme outlining formation and reactions of $[\{K(18\text{-}C\text{-}6)\}_2(^{tBu}pyrr_2pyr)Fe(N_2)]$ (2).

[a] *Department of Chemistry, University of Pennsylvania, 231 S 34th St, Philadelphia, PA 19104, USA. E-mail: mindiola@sas.upenn.edu*
[b] *Department of Chemistry & Pharmacy, Inorganic Chemistry, Friedrich-Alexander-Universität Erlangen – Nürnberg (FAU), Erlangen 91058, Germany. E-mail: karsten.meyer@fau.de*

† Electronic supplementary information (ESI) available: ESI contains complete experimental details and spectral data. CCDC 2377358–2377361. For ESI and crystallographic data in CIF or other electronic format see DOI: https://doi.org/10.1039/d4cc04127e

topologically nonlinear.[12] Such a geometry is retained upon further reduction to the formally Fe^0 complex [{K_2(18-C-6)}{(^{tBu}pyrr$_2$pyr)-Fe}$_2$(μ-N_2)] or *via* oxidative substitution of N_2 with chalcogenides.[13] The full extent of low oxidation state iron chemistry using the ^{tBu}pyrr$_2$pyr ligand platform, especially as it pertains to mononuclear complexes, has so far been unexplored. Treatment of 1 equiv. of **1** with four equivalents of 18-C-6 and two equivalents of KC_8 in toluene at room temperature resulted in the initial formation of a brown residue. Allowing the reaction to stir for an additional hour at room temperature led to the conversion of the brown residue to a dark purple solution. After filtration and concentration *in vacuo*, the solution was cooled to −35 °C overnight to afford [{K(18-C-6)}$_2$(^{tBu}pyrr$_2$pyr)Fe(N_2)] (**2**), which could be isolated in 79% yield as dark crystals (Scheme 1 and Fig. 1). The ^{1}H NMR spectrum of **2** shows seven paramagnetically broadened and shifted resonances indicative of a C_s symmetric system (Fig. S1, ESI†). A single-crystal X-ray diffraction study (sc-XRD) of **2** shows a (^{tBu}pyrr$_2$pyr)Fe scaffold with a terminal N_2 ligand occupying the fourth coordination site and capped by a {K(18-C-6)}$^+$ unit. The second {K(18-C-6)}$^+$ is coordinated to the pyridyl portion of the meridional ligand. The geometry at the formally Fe(0) center in **2** can best be described as seesaw with a $\angle N_{pyr}$–Fe–N_2 angle of 140.7(2)° and a τ_4 value of 0.51. The N_2 ligand has an N–N bond length of 1.147(6) Å and a signature stretch at 1851 cm^{-1} in the IR spectrum (Fig. S21, ESI†) implying significant activation of the N_2 ligand when compared to its free form (1.0975 Å, 2331 cm^{-1}).[14] The low energy vibration and elongated N–N bond for the N_2 ligand implies not only the metal ion but the N_2 ligand to be the likely locus of reduction.[15] While we cannot determine the Fe oxidation state of **2** with complete certainty, a significantly shortened Fe–N_2 bond length of 1.775(4) Å and solution state magnetic moment of 4.1 μ_B, measured by Evans Method in C_6D_6, which is above the expectation value for an S = 1 system, and implies contribution of a Fe^I atom and N_2-centered radical to the complicated electronic structure. In contrast to the bridging nature of [{K_2(18-C-6)(^{tBu}pyrr$_2$pyr)Fe}$_2$(μ-N_2)], we propose the mononuclear structure of **2** to derive from the addition of more equivalents of 18-crown-6.

Interested in the oxidative chemistry of **2**, we treated this species with one equivalent of bispinacolato diboron (B_2pin_2) in benzene expecting to observe reductive cleavage of the B–B bond. However, upon addition of the B_2pin_2, the reaction mixture gradually changed color from dark purple to red, and over 16 hours there was deposition of red crystals. A sc-XRD study on a single-crystal isolated from the reaction mixture confirms the structure to be instead the discrete phenyl salt [{K(18-C-6)}(^{tBu}pyrr$_2$pyr)Fe(C_6H_5)] (**3**) which was isolated in 61% yield. The solid-state structure of **3** shows a formally Fe^{II} ion with an Fe–C bond length of 2.068(1) Å resulting from benzene C–H activation. The $\angle N_{pyr}$–Fe–C_{Ar} angle is 123.88(5)° and the geometric index value of τ_4 = 0.74 is consistent with a distorted *cis*-divacant octahedral coordination geometry. A ^{1}H NMR spectroscopic study of these crystals in thf-d_8 shows 9 paramagnetically shifted and broadened resonances showing preservation of a C_s symmetric system in solution (Fig. S2, ESI†). A room temperature solution state magnetic moment of 4.8 μ_B, determined by Evans method, is close to the spin only value for an S = 2 system in accord with a high spin Fe^{II} ion in **3**. Examination of the supernatant from the reaction between **2** and B_2Pin_2 by ^{11}B NMR spectroscopy in thf-d_8 revealed 2 resonances at 30.97 ppm and 5.91 ppm (Fig. S9, ESI†). Resonances in these positions can be attributed to one trigonal planar and one pyramidal B atom as demonstrated by Marder and coworkers in a series of [{K(18-crown-6)}XB_2pin_2] molecules, where X = O^{t}Bu, OMe, and F.[16] In our case, the B-containing molecule could be crystallized out of a concentrated thf solution at −35 °C and its structure determined to be [{K(18-crown-6)}HB_2pin_2] (**4**). A sc-XRD structure of **4** clearly shows a HB_2pin_2 core with two distinctly different B centers as well as a {K(18-C-6)}$^+$ counter ion interacting with the hydride and nearby pinacolato oxygen (Fig. 1). ^{11}B NMR spectroscopy of the crystals also showed, as expected, 2 resonances, albeit at slightly different chemical shifts (Fig. S8, ESI†) when compared to the crude material. We attribute this discrepancy to the lack of paramagnetic impurities in the crystalline material contributing to a noncontact paramagnetic shift.[17] Transfer of a hydrogen atom to a borane has been reported before in the

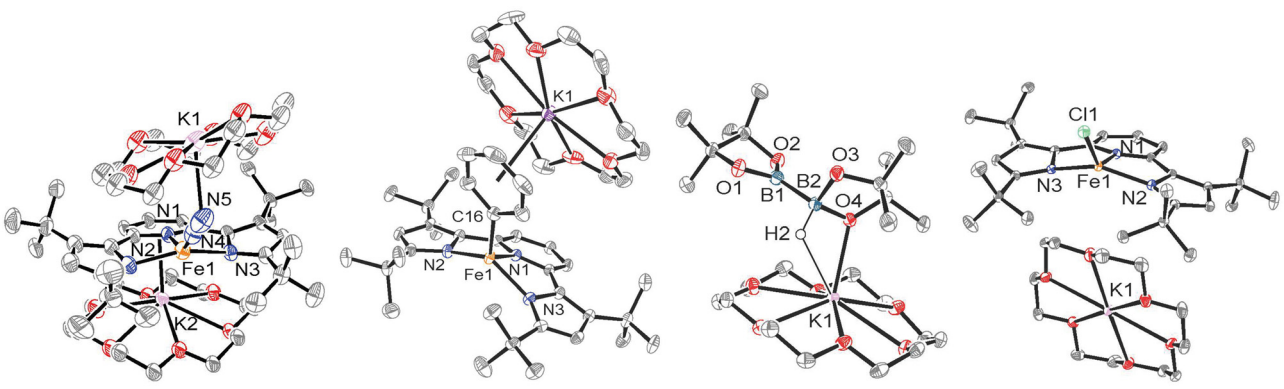

Fig. 1 ORTEP sc-XRD structures of complexes **2**, **3**, **4**, and **5** at 50% probability level. Residual solvent molecules and H atoms (with the exception of the hydride in compound **4**) have been omitted for clarity. Coordinated thf molecules coordinated to K^+ in compound **5** have been also omitted for clarity.

context of C–H activation at low valent iron centers, but diboron reagents have not been used to sponge out the hydride most likely stemming from heterolytic C–H bond cleavage.[5e,5g] Using other hydride acceptors such as imines and nitriles or other Lewis acids such as $B(C_6F_5)_3$ did not result in the formation of **3** (Fig. S13–S17, ESI†). We found that complex **3** could also be generated by reaction of **2** with fluorobenzene at room temperature (Scheme 1) in a manner similar to Holland's work using low valent Co complexes.[18] Unfortunately, our reaction was not quantitative thus resulting in formation of other intractable materials (Fig. S10, ESI†). Selective C–F bond activation is rare[19] and C–F bonds are known to be stable toward catalytic C–H borylation protocols.[8a,8c,8h,9c]

Having demonstrated that **2** could undergo C–H activation of benzene we next turned to delivering or functionalizing the phenyl moiety of **3**. Accordingly, treatment of **3** with one equivalent of ClBcat in thf-d_8 resulted in a new paramagnetic molecule when judged by ^{1}H NMR spectroscopy. ^{1}H and ^{11}B NMR spectroscopy confirmed that a second, diamagnetic species was formed, namely PhBCat (Fig. S19, ESI,† ^{11}B NMR δ = 32.6).[20] The paramagnetic product was identified to be [{K(18-C-6)(thf)$_2$}($^{t\text{Bu}}$pyrr$_2$pyr)FeCl] (**5**) using a combination of ^{1}H NMR, sc-XRD, solution magnetic susceptibility studies, as well as by an independent synthesis in 92% isolated yield *via* addition of 2 equiv. of Me_3SiCl to the N_2 precursor **1** (Scheme 1). A ^{1}H NMR spectrum in thf-d_8 is consistent with a plane of symmetry bisecting **5** given the observation of seven paramagnetically shifted and broadened resonances (Fig. S3, ESI†). A sc-XRD study on **5** shows the ($^{t\text{Bu}}$pyrr$_2$pyr)Fe core with a chloride ligand occupying the fourth coordination site and {K(18-crown-6)(thf)$_2$}$^+$ in the unit cell but not interacting with the iron complex. The Fe–Cl bond length is 2.2914(5) Å, which is longer than the Fe–Cl bond length of 2.1883(9) Å in the neutral ferric congener [($^{t\text{Bu}}$pyrr$_2$pyr)FeCl].[11] In the structure of **5** the $\angle N_{pyr}$–Fe–Cl angle is 135.34(3)° and the geometric index τ_4 value is 0.60, which makes this geometry best described as seesaw. A solution state magnetic moment of **5**, determined by Evans method, is 5.4 μ_B and is consistent with an S = 2 system.

In the interest of investigating the electronic structures of these mononuclear formally Fe^{II} ate complexes (**3** and **5**), ^{57}Fe Mössbauer spectroscopy and DC SQUID magnetometry measurements were performed on complex **5** as a representative example of this new class of compounds (Fig. 2). ^{57}Fe Mössbauer spectroscopy of **5** at 77 K shows a quadrupole doublet with an isomer shift of δ = 0.82 mm s^{-1}, a quadrupole splitting of ΔE_Q = 1.02 mm s^{-1}, and a linewidth of Γ_{FWHM} = 0.32 mm s^{-1}. These values are consistent with an S = 2 Fe^{II} ion on the $^{t\text{Bu}}$pyrr$_2$pyr ligand platform.[11,13,21] This spin state was further confirmed by a DC SQUID magnetometry study which showed a field-independent magnetic moment of 5.28 μ_B (averaged between two independently measured samples) at 300 K. Unfortunately, due to difficulties in scaling up the synthesis of **3**, we were unable to collect reliable ^{57}Fe Mössbauer spectroscopy and DC SQUID magnetometry measurements on this complex in order to directly compare with **5**. We can, however, be reasonably confident in our assignment of its oxidation and spin state as S = 2 Fe^{II} due to its solution state magnetic moment of 4.8 μ_B and similarities with **5** in its electronic absorption spectrum (Fig. S22 and S23, ESI†).

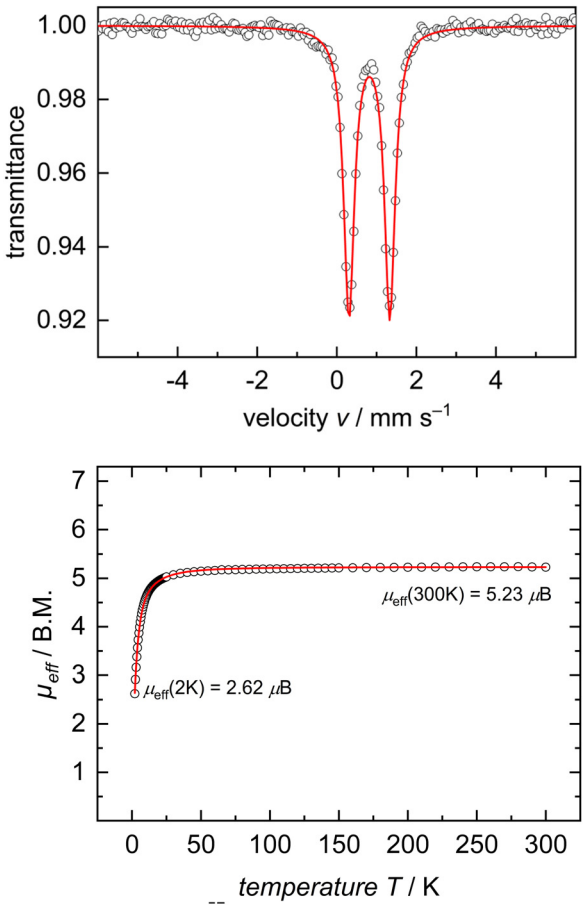

Fig. 2 (Top) Zero-field ^{57}Fe-Mössbauer spectrum of **5** (solid state, 77 K). Measured data were fit with parameters δ = 0.82 mm s^{-1}, ΔE_Q = 1.02 mm s^{-1}, and Γ_{FWHM} = 0.32 mm s^{-1}. (bottom) Temperature-dependent SQUID magnetization measurement of a powdered sample of **5** recorded from 2 to 300 K with an applied magnetic field of 1 T. Measured data were fit with parameters S = 2, TIP = 1023 × 10^{-6} emu, $|D|$ = 12 cm^{-1}, E/D = 0.14, and g_{av} = 2.14.

When complex **5** is reduced with an excess of KC_8 and one equivalent of 18-C-6 under an N_2 atmosphere, a gradual color change from red to dark purple is observed. Filtering the solution after one hour of reaction time and crystallization out of a concentrated toluene solution yields small black crystals that were identified as complex **2** by ^{1}H NMR spectroscopy (Fig. S20, ESI†), thus completing a synthetic cycle of benzene activation and borylation involving the Fe^0/Fe^{II} couple. Future work will involve attempts at rendering this system catalytic as well as expanding the substrate scope with the aim of site-selective C–H bond activation.

EZ synthesized the complexes, and wrote part of the manuscript. LP collected and analysed the Mössbauer and SQUID data. AK assisted with the synthesis of complexes. MRG solved and curated the crystal structures. KM and DJM provided funding and equipment for the project and helped compose the manuscript.

This work was supported by the U.S. Department of Energy, Office of Basic Energy Sciences (DOE-BES-DESC0023340) and the University of Pennsylvania (UPenn, D. J. M.), the Friedrich-Alexander-Universität Erlangen – Nürnberg, and the Alexander von Humboldt Foundation (K. M. and D. J. M.). A. K. thanks the Vagelos Integrated Program in Energy Research at UPenn for support.

Data availability

Data for this article including full synthetic procedures and characterization are available in the ESI.†

Conflicts of interest

There are no conflicts to declare.

References

1 (*a*) S. K. Bose, L. Mao, L. Kuehn, U. Radius, J. Nekvinda, W. L. Santos, S. A. Westcott, P. G. Steel and T. B. Marder, *Chem. Rev.*, 2021, **121**, 13238–13341; (*b*) I. F. Yu, J. W. Wilson and J. F. Hartwig, *Chem. Rev.*, 2023, **123**, 11619–11663; (*c*) R. Arevalo and P. J. Chirik, *J. Am. Chem. Soc.*, 2019, **141**, 9106–9123.
2 (*a*) M. Lersch and M. Tilset, *Chem. Rev.*, 2005, **105**, 2471–2526; (*b*) J. A. Labinger and J. E. Bercaw, *Nature*, 2002, **417**, 507–514; (*c*) B. A. Arndtsen, R. G. Bergman, T. A. Mobley and T. H. Peterson, *Acc. Chem. Res.*, 1995, **28**, 154–162; (*d*) A. E. Shilov and G. B. Shul'pin, *Chem. Rev.*, 1997, **97**, 2879–2932; (*e*) R. H. Crabtree, *J. Chem. Soc., Dalton Trans.*, 2001, 2437–2450.
3 (*a*) K. C. Nicolaou, P. G. Bulger and D. Sarlah, *Angew. Chem., Int. Ed.*, 2005, **44**, 4442–4489; (*b*) J. K. Stille, *Angew. Chem., Int. Ed. Engl.*, 1986, **25**, 508–524; (*c*) X. Chen, K. M. Engle, D. H. Wang and Y. Jin-Quan, *Angew. Chem., Int. Ed.*, 2009, **48**, 5094–5115.
4 N. Miyaura and A. Suzuki, *Chem. Rev.*, 1995, **95**, 2457–2483.
5 (*a*) S. Camadanli, R. Beck, U. Flörke and H.-F. Klein, *Organometallics*, 2009, **28**, 2300–2310; (*b*) M. V. Baker and L. D. Field, *J. Am. Chem. Soc.*, 1987, **109**, 2825–2826; (*c*) L. D. Field, R. W. Guest and P. Turner, *Inorg. Chem.*, 2010, **49**, 9086–9093; (*d*) S. Camadanli, R. Beck, U. Flörke and H.-F. Klein, *Organometallics*, 2009, **28**, 2300–2310; (*e*) A. Casitas, H. Krause, S. Lutz, R. Goddard, E. Bill and A. Fürstner, *Organometallics*, 2018, **37**, 729–739; (*f*) S. D. Ittel, C. A. Tolman, A. D. English and J. P. Jesson, *J. Am. Chem. Soc.*, 1976, **98**, 6073–6075; (*g*) S. F. McWilliams, D. L. J. Broere, C. J. V. Halliday, S. M. Bhutto, B. Q. Mercado and P. L. Holland, *Nature*, 2020, **584**, 221–226; (*h*) W. D. Jones, G. P. Foster and J. M. Putinas, *J. Am. Chem. Soc.*, 1987, **109**, 5047–5048; (*i*) M. K. Whittlesey, R. J. Mawby, R. Osman, R. N. Perutz, L. D. Field, M. P. Wilkinson and M. W. George, *J. Am. Chem. Soc.*, 1993, **115**, 8627–8637; (*j*) C. A. Tolman, S. D. Ittel, A. D. English and J. P. Jesson, *J. Am. Chem. Soc.*, 1979, **101**, 1742–1751; (*k*) A. K. Hickey, S. A. Lutz, C.-H. Chen and J. M. Smith, *Chem. Commun.*, 2017, **53**, 1245–1248.
6 ed. W. M. Haynes, D. R. Lide and T. J. Bruno, CRC Press, Boca Raton, FL, 97th edn, 2016, p. 19.
7 (*a*) K. M. Waltz, X. He, C. Muhoro and J. F. Hartwig, *J. Am. Chem. Soc.*, 1995, **117**, 11357–11358; (*b*) T. J. Mazzacano and N. P. Mankad, *Chem. Commun.*, 2015, **51**, 5379–5382; (*c*) K. M. Waltz, C. N. Muhoro and J. F. Hartwig, *Organometallics*, 1999, **18**, 3383–3393.
8 (*a*) L. Britton, J. H. Docherty, G. S. Nichol, A. P. Dominey and S. P. Thomas, *Chin. J. Chem.*, 2022, **40**, 2875–2881; (*b*) T. Dombray, C. G. Werncke, S. Jiang, M. Grellier, L. Vendier, S. Bontemps, J.-B. Sortais, S. Sabo-Etienne and C. Darcel, *J. Am. Chem. Soc.*, 2015, **137**, 4062–4065; (*c*) M. Kamitani, H. Kusaka and H. Yuge, *Chem. Lett.*, 2019, **48**, 898–901; (*d*) J.-L. Tu, A.-M. Hu, L. Guo and W. Xia, *J. Am. Chem. Soc.*, 2023, **145**, 7600–7611; (*e*) T. J. Mazzacano and N. P. Mankad, *J. Am. Chem. Soc.*, 2013, **135**, 17258–17261; (*f*) G. Yan, Y. Jiang, C. Kuang, S. Wang, H. Liu, Y. Zhang and J. Wang, *Chem. Commun.*, 2010, **46**, 3170–3172; (*g*) T. Kato, S. Kuriyama, K. Nakajima and Y. Nishibayashi, *Chem. – Asian J.*, 2019, **14**, 2097–2101; (*h*) H. Lee, T. He and S. P. Cook, *Org. Lett.*, 2023, **25**, 1–4; (*i*) M. Kamitani, *Chem. Commun.*, 2021, **57**, 13246–13258; (*j*) T. Hatanaka, Y. Ohki and K. Tatsumi, *Chem. – Asian J.*, 2010, **5**, 1657–1666.
9 (*a*) J. V. Obligacion, S. P. Semproni, I. Pappas and P. J. Chirik, *J. Am. Chem. Soc.*, 2016, **138**, 10645–10653; (*b*) J. V. Obligacion, S. P. Semproni and P. J. Chirik, *J. Am. Chem. Soc.*, 2014, **136**, 4133–4136; (*c*) T. P. Pabst and P. J. Chirik, *J. Am. Chem. Soc.*, 2022, **144**, 6465–6474.
10 S. R. Parmelee, T. J. Mazzacano, Y. Zhu, N. P. Mankad and J. A. Keith, *ACS Catal.*, 2015, **5**, 3689–3699.
11 K. Searles, S. Fortier, M. M. Khusniyarov, P. J. Carroll, J. Sutter, K. Meyer, D. J. Mindiola and K. G. Caulton, *Angew. Chem., Int. Ed.*, 2014, **53**, 14139–14143.
12 D. Sorsche, M. E. Miehlich, K. Searles, G. Gouget, E. M. Zolnhofer, S. Fortier, C.-H. Chen, M. Gau, P. J. Carroll, C. B. Murray, K. G. Caulton, M. M. Khusniyarov, K. Meyer and D. J. Mindiola, *J. Am. Chem. Soc.*, 2020, **142**, 8147–8159.
13 E. Zars, L. Gravogl, M. R. Gau, P. J. Carroll, K. Meyer and D. J. Mindiola, *Chem. Sci.*, 2023, **14**, 6770–6779.
14 (*a*) N. Hazari, *Chem. Soc. Rev.*, 2010, **39**, 4044–4056; (*b*) P. L. Holland, *Dalton Trans.*, 2010, **39**, 5415–5425.
15 J. B. Geri, J. P. Shanahan and N. K. Szymczak, *J. Am. Chem. Soc.*, 2017, **139**, 5952–5956.
16 S. Pietsch, E. C. Neeve, D. C. Apperley, R. Bertermann, F. Mo, D. Qiu, M. S. Cheung, L. Dang, J. Wang, U. Radius, Z. Lin, C. Kleeberg and T. B. Marder, *Chem. – Eur. J.*, 2015, **21**, 7082–7098.
17 J. D. Satterlee, *Concepts Magn. Reson.*, 1990, **2**, 69–79.
18 (*a*) T. R. Dugan, X. Sun, E. V. Rybak-Akimova, O. Olatunji-Ojo, T. R. Cundari and P. L. Holland, *J. Am. Chem. Soc.*, 2011, **133**, 12418–12421; (*b*) T. R. Dugan, J. M. Goldberg, W. W. Brennessel and P. L. Holland, *Organometallics*, 2012, **31**, 1349–1360.
19 (*a*) N. Toriumi, K. Yamashita and N. Iwasawa, *Chem. – Eur. J.*, 2021, **27**, 12635–12641; (*b*) Q. K. Kang, Y. Lin, Y. Li, L. Xu, K. Li and H. Shi, *Angew. Chem., Int. Ed.*, 2021, **60**, 20391–20399; (*c*) Y. Nakamura, N. Yoshikai, L. Ilies and E. Nakamura, *Org. Lett.*, 2012, **14**, 3316–3319; (*d*) Q.-K. Kang, Y. Lin, Y. Li, L. Xu, K. Li and H. Shi, *Angew. Chem., Int. Ed.*, 2021, **60**, 20391–20399; (*e*) D. Guijarro and M. Yus, *Tetrahedron*, 2000, **56**, 1135–1138.
20 D.-G. Yu and Z.-J. Shi, *Angew. Chem., Int. Ed.*, 2011, **50**, 7097–7100.
21 (*a*) E. Zars, L. Gravogl, M. Gau, P. J. Carroll, K. Meyer and D. J. Mindiola, *Inorg. Chem.*, 2022, **61**, 1079–1090; (*b*) D. Sorsche, M. E. Miehlich, E. M. Zolnhofer, P. J. Carroll, K. Meyer and D. J. Mindiola, *Inorg. Chem.*, 2018, **57**, 11552–11559.

